



## Structure guided P1' modifications of HEA derived $\beta$ -secretase inhibitors for the treatment of Alzheimer's disease

Holger Monenschein<sup>c,†</sup>, Daniel B. Horne<sup>a,\*</sup>, Michael D. Bartberger<sup>b</sup>, Stephen A. Hitchcock<sup>c,†</sup>, Thomas T. Nguyen<sup>a</sup>, Vinod F. Patel<sup>d,†</sup>, Lewis D. Pennington<sup>a</sup>, Wenge Zhong<sup>a</sup>

<sup>a</sup> Department of Chemistry Research and Discovery, Amgen Inc., One Amgen Center Drive, Thousand Oaks, CA 91320, USA

<sup>b</sup> Department of Molecular Structure, Amgen Inc., One Amgen Center Drive, Thousand Oaks, CA 91320, USA

<sup>c</sup> Envoy Therapeutics, 555 Heritage Drive, Jupiter, FL 33458, USA

<sup>d</sup> Sanofi-Aventis, 270 Albany Street, Cambridge, MA 02139, USA

### ARTICLE INFO

#### Article history:

Received 13 February 2012

Revised 5 April 2012

Accepted 10 April 2012

Available online 19 April 2012

#### Keywords:

A $\beta$  amyloid

Alzheimer's disease

Aspartyl protease

$\beta$ -secretase

BACE inhibitors

Hydroxyethylene derivatives

Protease inhibitors

### ABSTRACT

The synthesis and SAR of a series of BACE-1 hydroxyethyl amine inhibitors containing substitutions on a spirocyclobutyl moiety is described. Selectivity against cathepsin D, a related aspartyl protease with potential off target toxicity, and improved microsomal stability is exemplified.

© 2012 Elsevier Ltd. All rights reserved.

Alzheimer's disease (AD) is a neurodegenerative disease characterized by the progressive formation of insoluble amyloid plaques and neurofibrillary tangles in the brain. AD currently afflicts more than 27 million people worldwide, and the AD population is predicted to grow to 106 million by 2050,<sup>1</sup> creating a major economic and emotional burden on society. Currently only symptomatic treatments with modest effectiveness are available to treat AD.

$\beta$ -secretase (BACE-1) is a membrane bound aspartyl protease that initiates the amyloid cascade by cleavage of amyloid precursor protein (APP). The subsequent cleavage of the C-terminus of APP by gamma-secretase results in the formation of beta-amyloid peptides (A $\beta$ -40 and A $\beta$ -42), the principal components of amyloid plaques.<sup>2</sup> BACE-1 null mice are viable and do not produce amyloid plaques upon aging, suggesting that small-molecule inhibitors of BACE-1 would be potential disease modifying agents for AD.<sup>3</sup>

The identification of small-molecule inhibitors of BACE-1 has been the focus of many pharmaceutical and academic groups worldwide for the past 20 years.<sup>4</sup> Recently, potent non-peptidomimetic BACE-1 inhibitors with drug-like properties have been described.<sup>5</sup> However in large part, the successful design of

inhibitors has been hampered by the inherently poor pharmacokinetic properties of peptidomimetic compounds associated with inhibitors of aspartyl proteases coupled with the stringent physicochemical properties required to attain penetration of small-molecules across the blood–brain barrier.<sup>6</sup> As an additional challenge, selectivity against related aspartyl proteases is challenging due to high sequence homology of the active site, and in particular Cathepsin D (CatD) selectivity is desired in order to reduce potential off-target toxicity.<sup>7</sup>

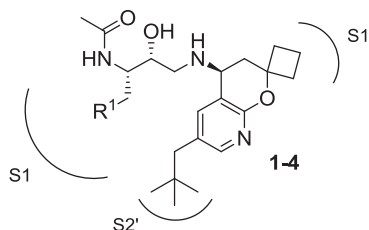
We have previously reported our design of orally efficacious hydroxyethylamine (HEA) inhibitors of BACE-1.<sup>7</sup> During the course of optimization of this series, we arrived at a potent series of peptidomimetic HEA inhibitors containing a spirocyclobutyl moiety (**1–4**, Table 1). Unfortunately, it was found that this series, although potent on BACE-1 and orally efficacious in the rat in vivo A $\beta$  lowering model, suffered from poor pharmacokinetics leading to poor projected human dose, high microsomal turnover, and had limited selectivity over CatD. Herein we describe our efforts towards optimization of the P1' spirocyclobutyl group to attain enhanced microsomal stability (hopefully leading to enhanced PK profiles), and superior CatD selectivity.

The in-house X-ray co-crystal structure<sup>8</sup> of **2** demonstrated the occupation of the S1' subsite by the cyclobutyl moiety.<sup>9</sup> However, it was observed that additional room existed for substitution in

\* Corresponding author.

E-mail address: [dhorne@amgen.com](mailto:dhorne@amgen.com) (D.B. Horne).

† Current address.

**Table 1**Selected rat and human microsomal stability data for spirocyclobutyl compounds **1–4** (S1–S2' indicate BACE-1 enzyme binding domains)

#	R <sup>1</sup>	RLM/HLM <sup>a</sup> (μL/min/mg)	BACE-1 IC <sub>50</sub> <sup>b</sup> (nM)	CatD IC <sub>50</sub> <sup>b</sup> (nM)	Selectivity (fold)
<b>1</b>	3-F-Ph	226/621	1	4	4.0
<b>2</b>	4-F-Ph	180/107	5	3	0.7
<b>3</b>	3,5-diF-Ph	186/921	7	2	0.3
<b>4</b>	CH=CH <sub>2</sub>	56/79	31	465	15.2

<sup>a</sup> RLM = rat liver microsomal stability; HLM = human liver microsomal stability. In vitro microsomal stability measured in a high-throughput automated format. Compound concentration = 1 μM. Microsomal protein concentration = 250 μg/mL.

<sup>b</sup> Average IC<sub>50</sub>'s of at least two independent experiments.

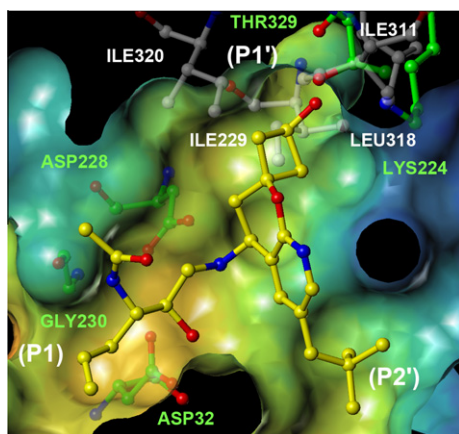
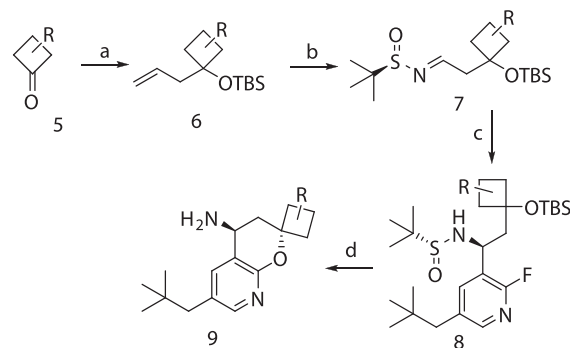


**Figure 1.** Model of *cis*-hydroxy compound **40** (yellow) docked into the active site of BACE-1 (cutaway surface view; flap residues not shown.) Key BACE-1 residues labeled in green, with relevant Cathepsin D S1' residues (transparent grey) labeled in white.

this region, giving rise to a potential avenue for additional BACE-1 potency and/or selectivity over CatD. In particular, the mismatched steric and polar characteristics of S1' sites of BACE-1 versus CatD were of note. Docking studies suggested that either van der Waals interactions, or even hydrogen bonding contacts if desired, could be made between substituents on the cyclobutyl ring and the nearby Thr329 and Lys224 residues of BACE-1. On the other hand, analogous docking into CatD (using literature structure 1LYB)<sup>10</sup> showed that such substitutions would be completely encapsulated by the bulkier and purely hydrophobic, 4-residue array consisting of Ile229, Ile311, Leu318, and Ile320 (Fig. 1) and thus polar and/or hydrophilic substitutions might be particularly desirable. Furthermore, since Met-ID studies suggested that the spirocyclobutyl subunit is a major site of oxidative metabolism, SAR studies were undertaken to attempt to improve stability of the inhibitors by reducing lipophilicity or blocking these potential sites of metabolism.

The synthesis of the required compounds was undertaken utilizing our established protocol for the synthesis of spirocyclobutyl containing 8-aza chroman amines (Scheme 1).<sup>9,11</sup> Alkylation of cyclobutanone **5** followed by protection of the secondary hydroxyl with TBSOTf gave allylcyclobutane **6**. The olefin was oxidatively cleaved by OsO<sub>4</sub> catalyzed dihydroxylation followed by sodium

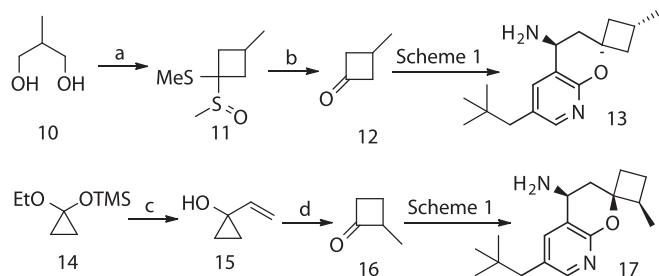


**Scheme 1.** Reagents and conditions: (a) (i) allylMgBr, THF, rt; (ii) TBSOTf, DIEA, CH<sub>2</sub>Cl<sub>2</sub>, rt; (b) (i) OsO<sub>4</sub>, NMO, *t*-BuOH/H<sub>2</sub>O/THF = 2/2/1, 6 h, rt; (ii) NaIO<sub>4</sub> *t*-BuOH/H<sub>2</sub>O/THF = 2/2/1, rt; (iii) CuSO<sub>4</sub>, (*R*)-2-methyl-2-propanesulfinamide, CH<sub>2</sub>Cl<sub>2</sub>, rt; (c) LiTMP, 2-fluoro-5-neopentylpyridine, THF, –78 °C, then 7, –78 °C to rt; (d) (i) TBAF, THF, rt, (ii) NaH, THF, 65 °C (iii) HCl (4 M in dioxane), THF.

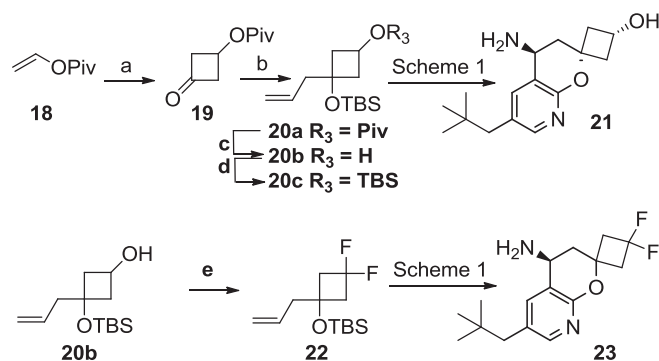
periodate to give an aldehyde which was condensed with Ellman's chiral sulfinamide<sup>12</sup> to give sulfonimine **7**. Diastereoselective addition of the aryl lithium typically gave >5:1 dr of the desired amine **8**. TBAF deprotection of the hydroxyl followed by NaH-promoted cyclization onto the fluoropyridine and deprotection of the amine with HCl gave the desired 8-azachroman amines **9**.

For the synthesis of 2- and 3-methyl substituted spirocyclobutyl chromans we first required 2- and 3-methylcyclobutanone (Scheme 2). The synthesis of 3-methylcyclobutanone **12** started from commercially available 2-methylpropane-1,3-diol **10** which was converted to a ditosylate, and then cyclized to dithiane **11** utilizing conditions similar to those described for cyclization of dibromoalkanes with methyl methylthiomethyl sulfoxide.<sup>13</sup> Acid-mediated cleavage afforded 3-methylcyclobutanone **12**. 2-Methylcyclobutanone **16** was prepared by methanolysis of (1-ethoxycyclopropoxy)trimethylsilane<sup>14</sup> **14** followed by addition of vinylmagnesium bromide to give vinyl cyclopropane **15**. Acid-facilitated cyclopropane rearrangement<sup>14</sup> gave 2-methylcyclobutanone **16**. The cyclobutanones were then carried forward using the generic procedure above (Scheme 1) to provide the 2- and 3-methylspirocyclobutylchromans **13** and **17**.

For the 3-hydroxy and 3,3-difluoro analogs, the synthesis began with the 2+2 cycloaddition of vinyl pivalate **18** with in situ generated dichloroketene to afford a 2,2-dichlorocyclobutanone, which upon zinc mediated reduction gave cyclobutanone **19** (Scheme 3). Alkylation with allyltrimethylsilane and TiCl<sub>4</sub> and protection



**Scheme 2.** Reagents and conditions: (a) (i) TsCl, Py, rt, 12 h, 81%; (ii) methylsulfanyl(methylthio)methane, *n*-BuLi;  $-10^{\circ}\text{C}$  to rt (b) HCl, distillation  $110\text{--}120^{\circ}\text{C}$ , 60% (c) (i) MeOH, rt, 62%; (ii)  $\text{H}_2\text{C}=\text{CHMgBr}$ , 70%; (d)  $\text{H}_2\text{SO}_4$ ,  $0^{\circ}\text{C}$ , 55%.



**Scheme 3.** Reagents and conditions: (a) (i) trichloroacetylchloride, Zn powder,  $\text{Et}_2\text{O}$ , rt, 100%; (ii) Zn powder, AcOH,  $0^{\circ}\text{C}$ , 85%; (b) (i) allyltrimethylsilane,  $\text{TiCl}_4$ ,  $0^{\circ}\text{C}$  to rt, 95%; (ii) TBSOTf, *i*-Pr<sub>2</sub>NEt,  $\text{CH}_2\text{Cl}_2$ , rt, 77%; (c) DIBAL-H,  $\text{CH}_2\text{Cl}_2$ ,  $-78^{\circ}\text{C}$ , 98% (d) TBSOTf, *i*-Pr<sub>2</sub>NEt,  $\text{CH}_2\text{Cl}_2$ , rt, 82%; (e) (i) Dess–Martin preiodinane,  $\text{NaHCO}_3$ ,  $\text{CH}_2\text{Cl}_2$ , 91%; (ii) (diethylamino)sulfurtrifluoride, 10% EtOH,  $\text{CH}_2\text{Cl}_2$ , rt, 28%.

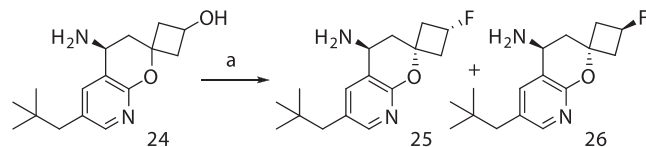
of the hydroxyl group as the *tert*-butyldimethylsilyl ether yielded **20a**. Protecting group switch from the pivalate to the silyl ether afforded disilyl ether **20c**, which was carried on (Scheme 1) to give the 2-hydroxyl chromans **21**. The 3,3-difluoro analog was prepared from **20a** by reductive removal of the pivalate protecting group to give 3-hydroxycyclobutane **20b**. Oxidation of the secondary alcohol to the ketone and transformation of the ketone to the 3,3-difluoro cyclobutane **22** was accomplished by DAST-mediated fluorination. The cyclobutane then intercepted intermediate **6** in the generic synthesis (Scheme 1) to give chroman **23**.

We prepared the 3-fluoro analogs from the 3-hydroxy chroman **24** by DAST mediated fluorination. The diastereomeric fluoro compounds were separated by silica gel chromatography to give **25** and **26** (Scheme 4).

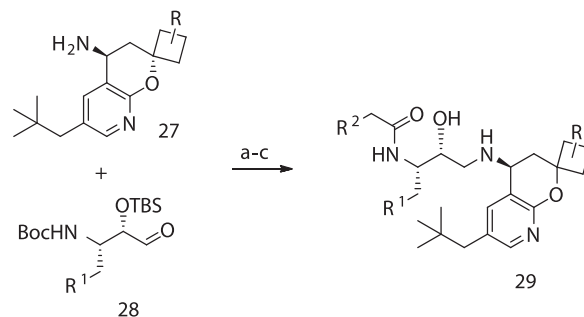
With the required chromans in hand, the conversion to final compounds was accomplished by means of the three step procedure below (Scheme 5). Reductive amination with the chroman **27** and aldehyde **28**, followed by global deprotection of the TBS ether and the Boc amine with HCl, and subsequent installation of the secondary amide with acetylimidazole (or EDCI and an acid) gave the required HEA compounds **29**.

2-methyl substituted analogs **30–33** were screened in BACE-1 and Cat D enzymatic assays and in vitro stability assessment was performed. We found that both CatD selectivity and microsomal stability in the 2-methyl substituted analogs **30–33** was disappointing (Table 2). Interestingly compounds **31** and **33** were substantially less active on BACE-1 showing a 2–3 order of magnitude loss of potency compared to the des-methyl compound **2**.

We found that the introduction of the 3-methyl group, preferably in the *cis* configuration, relative to the oxygen, (**35** and **37**, Table 3) significantly improved CatD selectivity when compared to the parent compounds (**2** and **3**, Table 1). The *trans*-compounds



**Scheme 4.** Reagents and conditions: (a) (diethylamino)sulfurtrifluoride,  $\text{CH}_2\text{Cl}_2$ ,  $75^{\circ}\text{C}$ , 71%.



**Scheme 5.** Reagents and conditions: (a)  $\text{NaBH}(\text{OAc})_3$ ,  $\text{CH}(\text{OEt})_3$ , EtOH, (b) HCl, MeOH/1,4-dioxane (c) acetylimidazole, *i*-Pr<sub>2</sub>NEt, DMF or EDCI, *i*-Pr<sub>2</sub>NEt,  $\text{R}^2\text{CH}_2\text{CO}_2\text{H}$ , DMF.

**34** and **36** showed 4–10 fold less CatD selectivity versus the *cis*-isomers. Unfortunately, average microsomal stability of the 3-methyl analogs was significantly worse than the parent compounds.

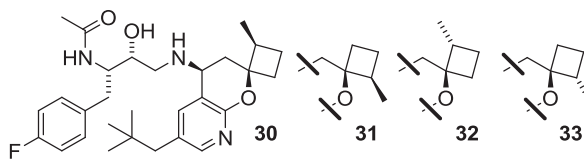
As an alternative to introducing methyl groups to the spirocyclobutyl ring, which are potential sites of metabolism, we switched our attention towards blocking sites of metabolism with fluorine atoms.<sup>15</sup> On average however, none of the 3-fluoro **38–41** or 3,3-difluoro **42** analogs offered significant stability improvement, and only moderate CatD selectivity was observed (Table 4).

In order to address the metabolic stability issues, we explored reducing lipophilicity while also blocking a potential site of metabolism. Thus we examined the 3-hydroxyl substituted analogs **43–46** (Table 5). In contrast to the 3-methyl analogs we found that the introduction of the 3-hydroxy group had a more pronounced affect on CatD selectivity, in excess of 100 fold. The stereochemical *cis* preference (*cis*-**44** versus *trans*-**43**) tracked nicely with the previously established 3-methyl SAR. The selectivity came at a price however, and microsomal stability in the series was still relatively poor, particularly in RLM. One explanation for the decreased stability could be that the sterically exposed 3-hydroxy group may be prone to metabolic oxidation. In addition, examination of the P-gp efflux potential of the molecules in P-gp expressing LLC-PK<sub>1</sub> cells (pig kidney epithelial cells) showed that compound **44** was poorly permeable. Compounds **45** and **46** were made in attempt to shield the amide NH by an intramolecular hydrogen bond to increase permeability,<sup>16</sup> but did not result in better efflux properties.

Combination of the preferred *cis*-3-hydroxyspirocyclobutyl substitution with the moderately CatD selective and microsomal stable P1-allyl group compound **4** (Table 1) gave compound **47** which had >8500 fold CatD selectivity (Table 5). Microsomal stability was also significantly improved. However, efflux remained a liability and the molecule was poorly permeable.

In light of the favorable profiles of compounds **44** and **47**, in regards to potency and CatD selectivity, they were advanced to in vivo rat PD efficacy studies.<sup>17</sup> The efficacy studies with **44** and **47** at 100 and 30 mg/kg doses (PO) showed negligible (<15%) lowering of A $\beta$ 40 in cerebral spinal fluid in rat after 4 h and low plasma concentrations of the parent compounds (**44** = 0.012  $\mu\text{M}$ , 100 mg/kg, 4 h post dose; **47** = 0.009  $\mu\text{M}$ , 30 mg/kg, 4 h post dose) Subsequent profiling revealed that compound **44** suffered from poor in vivo PK (rat IV clearance = 7.6 L/h/kg) as well as poor passive

**Table 2**  
Effect of 2-methyl substitution on microsomal stability and CatD selectivity

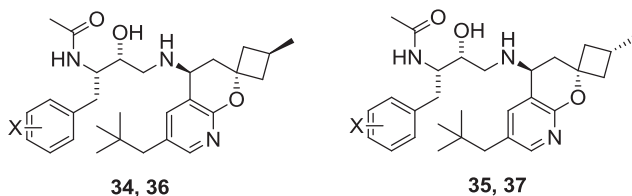


#	RLM/HLM <sup>a</sup> (μL/min/mg)	BACE-1 IC <sub>50</sub> <sup>b</sup> (nM)	CatD IC <sub>50</sub> <sup>b</sup> (nM)	Selectivity (fold)
<b>30</b>	236/232	7	5	0.7
<b>31</b>	399/829	30500	20500	0.7
<b>32</b>	227/68	29	46	1.6
<b>33</b>	399/590	>40000	>40000	—

<sup>a</sup> RLM = rat liver microsomal stability; HLM = human liver microsomal stability. In vitro microsomal stability measured in a high-throughput automated format. Compound concentration = 1 μM. Microsomal protein concentration = 250 μg/mL.

<sup>b</sup> Average IC<sub>50</sub>'s of at least two independent experiments.

**Table 3**  
Effect of 3-methyl substitution on microsomal stability and CatD selectivity

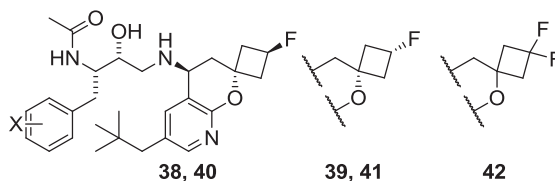


#	X	RLM/HLM <sup>a</sup> (μL/min/mg)	BACE-1 IC <sub>50</sub> <sup>b</sup> (nM)	CatD IC <sub>50</sub> <sup>b</sup> (nM)	Selectivity (fold)
<b>34</b>	4-F	399/246	9	8	0.9
<b>35</b>	4-F	451/108	4	38	9.5
<b>36</b>	3,4-diF	921/775	0.7	4	6.2
<b>37</b>	3,4-diF	706/399	0.7	17	25

<sup>a</sup> RLM = rat liver microsomal stability; HLM = human liver microsomal stability. In vitro microsomal stability measured in a high-throughput automated format. Compound concentration = 1 μM. Microsomal protein concentration = 250 μg/mL.

<sup>b</sup> Average IC<sub>50</sub>'s of at least two independent experiments.

**Table 4**  
Effect of 3-fluoro and 3-gem-difluoro substitution on microsomal stability and CatD selectivity



#	X	RLM/HLM <sup>a</sup> (μL/min/mg)	BACE-1 IC <sub>50</sub> <sup>b</sup> (nM)	CatD IC <sub>50</sub> <sup>b</sup> (nM)	Selectivity (fold)
<b>38</b>	4-F	370/223	9	8	0.9
<b>39</b>	4-F	411/240	6	14	2.3
<b>40</b>	3-F	492/829	2	12	6
<b>41</b>	3-F	447/706	2	22	11
<b>42</b>	4-F	399/408	8	11	1.4

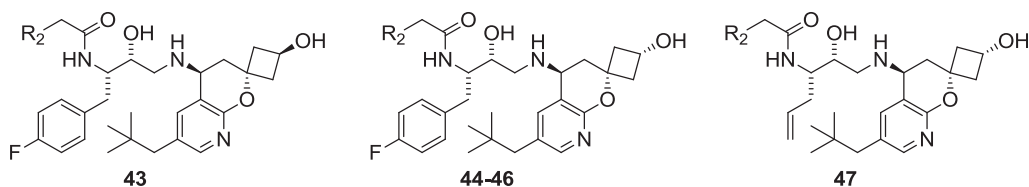
<sup>a</sup> RLM = rat liver microsomal stability; HLM = human liver microsomal stability. In vitro microsomal stability measured in a high-throughput automated format. Compound concentration = 1 μM. Microsomal protein concentration = 250 μg/mL.

<sup>b</sup> Average IC<sub>50</sub>'s of at least two independent experiments.

permeability (Papp A to B =  $3.2 \times 10^{-6}$  cm/sec). Although compound **47** initially appeared promising due to the inherent microsomal stability compared to **44**, the poor results in the rat PD efficacy study and low plasma concentration likely also resulted from poor pharmacokinetic properties. In addition, the poor permeability of these compounds makes the prospect of these inhibitors crossing the blood–brain barrier to inhibit BACE-1 in the brain unlikely, providing further deemphasis of these particular compounds.

Despite a committed and focused effort addressing the inherent low microsomal stability and the correlated unfavorable in vivo pharmacokinetic profile showing high clearance and low oral bioavailability of this chemical series, it proved to be rather difficult to obtain analogs containing both high intrinsic stability coupled with good selectivity over CatD simply by substitution of the cyclobutyl ring. A notable exception to this was compound **47**, which was stable in microsomes, potent, and selective, but suffered from high efflux and poor PK properties in the rat in vivo Aβ lowering model.

**Table 5**  
Effect of 3-hydroxy substitution on microsomal stability and CatD selectivity



#	R <sub>2</sub>	metabolic stability RLM/HLM <sup>a</sup> (μL/min/mg)	BACE-1 IC <sub>50</sub> <sup>b</sup> (nM)	HEK IC <sub>50</sub> <sup>b,c</sup> (nM)	CatD IC <sub>50</sub> <sup>b</sup> (nM)	CatD selectivity (fold)	Papp <sup>d</sup> (×10 <sup>-6</sup> cm/ sec)	Pgp-Efflux <sup>e</sup>	
								Rat	Human
43	H	228/90	14	41	1650	115	2.6	–	21.5
44	H	706/34	3	5	577	184	4.3	>50	13.5
45	OMe	682/115	2	8	695	285	6.5	–	35.8
46	F	775/65	4	10	347	81	6.4	–	>50
47	H	56/<14	5	27	>40000	>8500	<2	>50	>50

<sup>a</sup> RLM = rat liver microsomal stability; HLM = human liver microsomal stability. In vitro microsomal stability measured in a high-throughput automated format. Compound concentration = 1 μM. Microsomal protein concentration = 250 μg/mL.

<sup>b</sup> Average IC<sub>50</sub>'s of at least two independent experiments.

<sup>c</sup> Cell potency measured in human embryonic kidney (HEK293) cells stably expressing APP.

<sup>d</sup> Apparent permeability measured in parental LLC-PK1 cells.

<sup>e</sup> Efflux measured in LLC-PK1 cells transfected with rat MDR1A/1B or human MDR1 and reported as a ratio of (B to A)/(A to B).

Further efforts describing additional compounds with more extensive substitutions and resulting in improved PK, and in vivo efficacy than that described in this manuscript will be reported subsequently.

## References and notes

- Brookmeyer, R.; Johnson, E.; Ziegler-Graham, H.; Arrighi, H. M. *Alzheimer's & Dementia: J. Alzheimer's Assoc.* **2007**, *3*, 186.
- Vassar, R.; Bennett, B. D.; Babu-Khan, S.; Kahn, S.; Mendiaz, E. A.; Denis, P.; Teplow, D. B.; Ross, S.; Amarante, P.; Loeloff, R.; Luo, Y.; Fisher, S.; Fuller, J.; Edenson, S.; Lile, J.; Jarosinski, M. A.; Biere, A. L.; Curran, E.; Burgess, T.; Louis, J. C.; Collins, F.; Treanor, J.; Rogers, G.; Citron, M. *Science* **1999**, *286*, 735.
- Roberds, S. L.; Anderson, J.; Basi, G.; Bienkowski, M. J.; Branstetter, D. G.; Chen, K. S.; Freedman, S. B.; Frigon, N. L.; Games, D.; Hu, K.; Johnson-Wood, K.; Kappenman, K. E.; Kawabe, T. T.; Kola, I.; Kuehn, R.; Lee, M.; Liu, W.; Motter, R.; Nichols, N. F.; Power, M.; Robertson, D. W.; Schenk, D.; Schoor, M.; Shopp, G. M.; Shuck, M. E.; Sinha, S.; Svensson, K. A.; Tatsuno, G.; Tintrop, H.; Wijsman, J.; Wright, S.; McConlogue, L. *Hum. Mol. Genet.* **2001**, *10*, 1317.
- (a) Silvestri, R. *Med. Res. Rev.* **2008**, *29*, 295; (b) Stachel, S. *J. Drug Dev. Res.* **2009**, *70*, 101; (c) Hamada, Y.; Kiso, Y. *Exp. Opin. Drug Disc.* **2009**, *4*, 391.
- (a) Zhu, Z.; Sun, Z.; Ye, Y.; Voigt, J.; Strickland, C.; Smith, E. M.; Cumming, J.; Wang, L.; Wong, J.; Wand, Y.; Wyss, D. F.; Chen, X.; Kuvelkar, R.; Kennedy, M. E.; Favreau, L.; Parker, E.; McKittrick, B. A.; Stamford, A.; Czarniecki, M.; Greenlee, W.; Hunter, J. C. *J. Med. Chem.* **2010**, *53*, 951; (b) May, P. C.; Dean, R. A.; Lowe, S. L.; Martenyi, F.; Sheehan, S. M.; Boggs, L. N.; Monk, S. A.; Mathes, B. M.; Mergott, D. J.; Watson, B. M.; Stout, S. L.; Timm, D. E.; Smith-LaBell, E.; Gonzales, C. R.; Nakano, M.; Jhee, S. S.; Yen, M.; Ereshefsky, L.; Lindstrom, T. D.; Calligaro, D. O.; Cocke, P. J.; Hall, D. G.; Friedrich, S.; Citron, M.; Audia, J. E. *J. Neurosci.* **2011**, *31*, 16507.
- Hitchcock, S. A.; Pennington, L. D. *J. Med. Chem.* **2006**, *49*, 7559.
- Shacka, J. J.; Roth, K. A. *Autophagy* **2007**, *3*, 474.
- Coordinates for the complex of BACE-1 with inhibitor 2 have been deposited in the Protein Data Bank under PDB ID Code 4DUS.
- Kaller, M.R.; Harried, S.S.; Albrecht, B.; Amarante, P.; Babu-Khan, S.; Bartberger, M.D.; Brown, J.; Brown, R.; Chen, K.; Chen, Y.; Citron, M.; Croghan, M.D.; Graceffa, R.; Hickman, D.; Judd, T.; Kriemen, C.; La, D.; Li, V.; Lopez, P.; Luo, Y.; Masse, C.; Monenschein, H.; Nguyen, T.T.; Pennington, L.; San Miguel, T.; Sickmier, E.A.; Wahl, R.C.; Weiss, M.M.; Wen, P.H.; Williamson, T.; Wood, S.; Xue, M.; Yang, B.H.; Zhang, J.; Patel, V.F.; Zhong, W.; Hitchcock, S. *Med. Chem. Lett.* 2012, in press.
- Baldwin, E. T.; Bhat, T. N.; Gulnik, S.; Hosur, M. V.; Sowder, R. C.; Cachau, J.; Collins, J.; Silva, A. M.; Erickson, J. W. *Proc. Natl. Acad. Sci. U.S.A.* **1993**, *90*, 6796.
- (a) Zhong, W.; Hitchcock, S.; Patel, V.F.; Croghan, M.; Dineen, T.; Harried, S.; Horne, D.; Judd, T.; Kaller, M.; Kreiman, C.; Lopez, P.; Monenschein, H.; Nguyen, T.; Weiss, M.; Xue, Q.; Yang, B. PCT Int. Appl. WO2008147547, 2008.; (b) Zhong, W.; Hitchcock, S.; Patel, V.F.; Croghan, M.; Dineen, T.; Horne, D.; Kaller, M.; Kreiman, C.; Lopez, P.; Monenschein, H.; Nguyen, T.; Pennington, L.; Xue, Q.; Yang, B. PCT Int. Appl. WO2008147544, 2008.; (c) Zhong, W. et al. PCT Int. Appl. WO2007061670, 2007.
- Liu, G.; Cogan, D. A.; Ellman, J. A. *J. Am. Chem. Soc.* **1997**, *119*, 9913.
- Ogura, K.; Yamashita, M.; Suzuki, M.; Tsuchihashi, G. *Tetrahedron Lett.* **1974**, *15*, 3653.
- Girard, C.; Amice, P.; Barnier, J. P.; Conia, J. M. *Tetrahedron Lett.* **1974**, *15*, 3329.
- Hagmann, W. K. *J. Med. Chem.* **2008**, *51*, 4359.
- (a) Ettore, A.; D'Andrea, P.; Mauro, S.; Porcelloni, M.; Rossi, C.; Altamura, M.; Catalioto, R. M.; Giuliani, S.; Maggi, C. A.; Fattori, D. *BMCL* **2011**, *21*; (b) Kuhn, B.; Mohr, P.; Stahl, M. *J. Med. Chem.* **2010**, *53*, 2601; (c) Ashwood, V. A.; Field, M. J.; Horwell, D. C.; Julien-Larose, C.; Lewthwaite, R. A.; McCleary, S.; Pritchard, M. C.; Raphy, J.; Singh, L. *J. Med. Chem.* **2001**, *44*, 2276.
- Pharmacodynamic assay: Male Sprague-Dawley rats (175–200 g) were purchased from Harlan and were maintained on a 12 h light/dark cycle with unrestricted access to food and water until use. Rats were administered compound by oral gavage at the appropriate dose (5 rats/dose group). Rats were euthanized with CO<sub>2</sub> inhalation for 2 min and cisterna magna was quickly exposed by removing the skin and muscle above it. CSF (50–100 μl) was collected with a 30 gauge needle through the dura membrane covering the cisterna magna. Blood was withdrawn by cardiac puncture and plasma obtained by centrifugation for drug exposures. Brains were removed and, along with the CSF, immediately frozen on dry ice and stored at –80 °C until use. The frozen brains were subsequently homogenized in 10 volumes of (w/v) of 0.5% Triton X-100 in TBS with protease inhibitors. The homogenates were centrifuged at 100,000 rpm for 30 min at 4 °C. The supernatants were analyzed for Aβ<sub>40</sub> levels by immunoassay as follows: Meso Scale 96-well avidin plates were coated with Biotin-4G8 (Covance) and detected with Ruthenium-labeled Fab specific for Aβ<sub>40</sub>. Plates were read in MSD Sector6000 imager according to manufacturer's recommended protocol (Meso Scale Discovery, Inc.). Aβ<sub>40</sub> concentrations were plotted using Graphpad Prism and analyzed by one-way ANOVA followed by Dunnett's multiple comparison analysis to compare drug-treated animals to vehicle-treated controls.